# Probing the Repulsive Core of the Nucleon-Nucleon Interaction via the ⁴He(e,e′pN) Triple-Coincidence Reaction

I. Korover,[1] N. Muangma,[2] O. Hen,[1] R. Shneor,[1] V. Sulkosky,[2,3] A. Kelleher,[2] S. Gilad,[2] D. W. Higinbotham,[4] E. Piasetzky,[1]
J. W. Watson,[5] S. A. Wood,[4] P. Aguilera,[7] Z. Ahmed,[6] H. Albataineh,[8] K. Allada,[9] B. Anderson,[5]
D. Anez,[10] K. Aniol,[11] J. Annand,[12] W. Armstrong,[13] J. Arrington,[14] T. Averett,[15] T. Badman,[16] H. Baghdasaryan,[17]
X. Bai,[18] A. Beck,[19] S. Beck,[19] V. Bellini,[20] F. Benmokhtar,[21] W. Bertozzi,[2] J. Bittner,[3] W. Boeglin,[22] A. Camsonne,[4]
C. Chen,[23] J.-P. Chen,[4] K. Chirapatpimol,[17] E. Cisbani,[24] M. M. Dalton,[17] A. Daniel,[25] D. Day,[17] C. W. de Jager,[4,17]
R. De Leo,[26] W. Deconinck,[2] M. Defurne,[27] D. Flay,[13] N. Fomin,[28] M. Friend,[21] S. Frullani,[24] E. Fuchey,[13] F. Garibaldi,[24]
D. Gaskell,[4] R. Gilman,[29,4] O. Glamazdin,[30] C. Gu,[31] P. Gueye,[23] D. Hamilton,[12] C. Hanretty,[32] J.-O. Hansen,[4]
M. Hashemi Shabestari,[17] T. Holmstrom,[3] M. Huang,[33] S. Iqbal,[11] G. Jin,[17] N. Kalantarians,[34] H. Kang,[35] M. Khandaker,[4]
J. LeRose,[4] J. Leckey,[36] R. Lindgren,[17] E. Long,[16] J. Mammei,[37] D. J. Margaziotis,[11] P. Markowitz,[22]
A. Marti Jimenez-Arguello,[38] D. Meekins,[4] Z. Meziani,[13] R. Michaels,[4] M. Mihovilovic,[39] P. Monaghan,[2,23]
C. Munoz Camacho,[38] B. Norum,[17] ,[40] K. Pan,[2] S. Phillips,[16] I. Pomerantz,[1,41] M. Posik,[13] V. Punjabi,[42] X. Qian,[33]
Y. Qiang,[33] X. Qiu,[43] A. Rakhman,[6] P. E. Reimer,[14] S. Riordan,[17,44] G. Ron,[45] O. Rondon-Aramayo,[4] A. Saha,[4,*]
E. Schulte,[29] L. Selvy,[5] A. Shahinyan,[46] S. Sirca,[47] J. Sjoegren,[12] K. Slifer,[16] P. Solvignon,[4] N. Sparveris,[13] R. Subedi,[17]
W. Tireman,[48] D. Wang,[17] L. B. Weinstein,[8] B. Wojtsekhowski,[4] W. Yan,[49] I. Yaron,[1] Z. Ye,[17] X. Zhan,[2] J. Zhang,[4]
Y. Zhang,[29] B. Zhao,[15] Z. Zhao,[17] X. Zheng,[17] P. Zhu,[49] and R. Zielinski[16]

(Jefferson Lab Hall A Collaboration)

[1]*Tel Aviv University, Tel Aviv 69978, Israel*
[2]*Massachusetts Institute of Technology, Cambridge, Massachusetts 02139, USA*
[3]*Longwood University, Farmville, Virginia 23909, USA*
[4]*Thomas Jefferson National Accelerator Facility, Newport News, Virginia 23606, USA*
[5]*Kent State University, Kent, Ohio 44242, USA*
[6]*Syracuse University, Syracuse, New York 13244, USA*
[7]*Institut de Physique Nucléaire (UMR 8608), CNRS/IN2P3—Université Paris-Sud, F-91406 Orsay Cedex, France*
[8]*Old Dominion University, Norfolk, Virginia 23529, USA*
[9]*University of Kentucky, Lexington, Kentucky 40506, USA*
[10]*Saint Mary's University, Halifax, Nova Scotia, Canada*
[11]*California State University, Los Angeles, Los Angeles, California 90032, USA*
[12]*University of Glasgow, Glasgow G12 8QQ, Scotland, United Kingdom*
[13]*Temple University, Philadelphia, Pennsylvania 19122, USA*
[14]*Physics Division, Argonne National Laboratory, Argonne, Illinois 60439, USA*
[15]*College of William and Mary, Williamsburg, Virginia 23187, USA*
[16]*University of New Hampshire, Durham, New Hampshire 03824, USA*
[17]*University of Virginia, Charlottesville, Virginia 22904, USA*
[18]*China Institute of Atomic Energy, Beijing, China*
[19]*Nuclear Research Center Negev, Beer-Sheva, Israel*
[20]*Universita di Catania, Catania, Italy*
[21]*Carnegie Mellon University, Pittsburgh, Pennsylvania 15213, USA*
[22]*Florida International University, Miami, Florida 33199, USA*
[23]*Hampton University, Hampton, Virginia 23668, USA*
[24]*INFN, Sezione Sanità and Istituto Superiore di Sanità, 00161 Rome, Italy*
[25]*Ohio University, Athens, Ohio 45701, USA*
[26]*INFN, Sezione di Bari and University of Bari, I-70126 Bari, Italy*
[27]*CEA Saclay, F-91191 Gif-sur-Yvette, France*
[28]*University of Tennessee, Knoxville, Tennessee 37996, USA*
[29]*Rutgers, The State University of New Jersey, Piscataway, New Jersey 08855, USA*
[30]*Kharkov Institute of Physics and Technology, Kharkov 61108, Ukraine*
[31]*Los Alamos National Laboratory, Los Alamos, New Mexico 87545, USA*
[32]*Florida State University, Tallahassee, Florida 32306, USA*
[33]*Duke University, Durham, North Carolina 27708, USA*
[34]*University of Texas, Houston, Texas 77030, USA*
[35]*Seoul National University, Seoul, Korea*

[36]*Indiana University, Bloomington, Indiana 47405, USA*
[37]*Virginia Polytechnic Institute and State University, Blacksburg, Virginia 24061, USA*
[38]*Université Blaise Pascal/IN2P3, F-63177 Aubière, France*
[39]*Jozef Stefan Institute, Ljubljana, Slovenia*
[40]*Mississippi State University, Mississippi State, Mississippi 39762, USA*
[41]*The University of Texas at Austin, Austin, Texas 78712, USA*
[42]*Norfolk State University, Norfolk, Virginia 23504, USA*
[43]*Lanzhou University, Lanzhou, China*
[44]*University of Massachusetts, Amherst, Massachusetts 01006, USA*
[45]*Racah Institute of Physics, Hebrew University of Jerusalem, Jerusalem, Israel*
[46]*Yerevan Physics Institute, Yerevan 375036, Armenia*
[47]*University of Ljubljana, Ljubljana, Slovenia*
[48]*Northern Michigan University, Marquette, Michigan 49855, USA*
[49]*University of Science and Technology, Hefei, China*

We studied simultaneously the $^4\mathrm{He}(e, e'p)$, $^4\mathrm{He}(e, e'pp)$, and $^4\mathrm{He}(e, e'pn)$ reactions at $Q^2 = 2(\mathrm{GeV}/c)^2$ and $x_B > 1$, for an $(e, e'p)$ missing-momentum range of 400 to 830 MeV/$c$. The knocked-out proton was detected in coincidence with a proton or neutron recoiling almost back to back to the missing momentum, leaving the residual $A = 2$ system at low excitation energy. These data were used to identify two-nucleon short-range correlated pairs and to deduce their isospin structure as a function of missing momentum, in a region where the nucleon-nucleon ($NN$) force is expected to change from predominantly tensor to repulsive. The abundance of neutron-proton pairs is reduced as the nucleon momentum increases beyond $\sim$500 MeV/$c$. The extracted fraction of proton-proton pairs is small and almost independent of the missing momentum. Our data are compared with calculations of two-nucleon momentum distributions in $^4$He and discussed in the context of probing the elusive repulsive component of the $NN$ force.

The stability of atomic nuclei is due to a delicate interplay between the long-range attraction that binds nucleons and the short-range repulsion that prevents the collapse of the system. In between, the dominant scalar part of the nucleon-nucleon force almost vanishes and the interaction is dominated by the tensor force, which depends on the spin orientations and the relative orbital angular momentum of the nucleons.

Recent high-momentum-transfer triple-coincidence $^{12}\mathrm{C}(e, e'pN)$ and $^{12}\mathrm{C}(p, 2pn)$ measurements [1–4] have shown that nucleons in the nuclear ground state form pairs with large relative momentum and small center-of-mass (c.m.) momentum, where large and small are relative to the Fermi momentum of the nucleus. We refer to these pairs as short-range correlated (SRC) pairs [5–7]. When the missing momentum (the knocked-out proton initial momentum in the absence of final state interactions) is in the range of 300–600 MeV/$c$, these pairs were found to dominate the high-momentum tails of the nuclear wave functions, with neutron-proton ($np$) pairs nearly 20 times more prevalent than proton-proton ($pp$) pairs, and by inference neutron-neutron ($nn$) pairs. This is due to the strong dominance of the $NN$ tensor interaction at the probed sub-Fermi distances [8–10].

The association of the small $^{12}\mathrm{C}(e, e'pp)/^{12}\mathrm{C}(e, e'pn)$ ratio at $(e, e'p)$ missing momenta of 300–600 MeV/$c$, with

dominance of the $NN$ tensor force, leads naturally to the quest for increasing missing momenta. This allows the search for pairs at distances in which the nuclear force changes from being predominantly tensor to the essentially unexplored repulsive interaction. We report here on a simultaneous measurement of the $^4\mathrm{He}(e, e'p)$, $^4\mathrm{He}(e, e'pp)$ and $^4\mathrm{He}(e, e'pn)$ reactions at $(e, e'p)$ missing momenta from 400 to 830 MeV/$c$. The observed changes in the isospin composition of the SRC pairs as a function of the missing momentum are presented, discussed, and compared to calculations.

The experiment was performed in Hall A of Jefferson Laboratory (JLab) using a 4 $\mu$A electron beam with an energy of 4.454 GeV incident on a 20-cm-long high pressure $^4$He gas target (13 atm, 20 K, 0.033 g/cm$^3$) contained in an 8-cm-diameter, 20-cm-long aluminum cylinder.

The two Hall A high-resolution spectrometers (HRS) [11] were used to identify $^4\mathrm{He}(e, e'p)$ events. Scattered electrons were detected in the left HRS (L-HRS) at a central scattering angle of 20.3° and momentum of 3.602 GeV/$c$. This setup corresponds to the quasi-free knockout of a single proton with transferred three-momentum $|\vec{q}| \approx 1.64$ GeV/$c$, transferred energy $\omega \approx 0.86$ GeV, the negative four-momentum transfer squared $Q^2 \approx 2(\mathrm{GeV}/c)^2$, and $x_B \equiv (Q^2/2m_p\omega) \approx 1.2$, where $m_p$ is the proton mass. Knocked-out protons were detected

using the right HRS (R-HRS), which was set at three different central angles and momenta: (33.5°, 1.38 GeV/$c$), (29°, 1.3 GeV/$c$), and (24.5°, 1.19 GeV/$c$). These kinematical settings correspond to $(e, e'p)$ central missing momenta $\vec{p}_{\text{miss}} = \vec{p}_p - \vec{q})$ values of 500 MeV/$c$, 625 MeV/$c$, and 750 MeV/$c$, respectively, covering a missing-momentum range of 400–830 MeV/$c$ with overlap between the three different settings.

The $^4$He$(e, e'p)$ events were selected by placing a $\pm 3\sigma$ cut around the $\sigma = 0.6$ ns coincidence timing peak. The fraction of random events inside the time window increased from 1% at the lowest missing momentum measurement to 9% at the highest. The other cuts on the $(e, e'p)$ data were the nominal HRS phase-space cuts on momentum ($|\Delta p/p| \leq 0.045$) and angles ($\pm 60$ mrad vertical, $\pm 30$ mrad horizontal). To reduce the random-coincidence background, a cut on the target-reconstructed vertex ensured that both the electron and the proton emerged from the same place within $\pm 3$ cm. The $\Delta(1232)$ excitation was excluded by a cut on the quasi elastic $(e, e'p)$ peak, as in Ref. [12].

For highly correlated pairs, the missing momentum of the $A(e, e'p)$ reaction is expected to be balanced almost entirely by a single recoiling nucleon. A large acceptance spectrometer (BigBite) followed by a neutron detector (HAND) with a matching solid angle was used to detect correlated recoiling protons or neutrons. The experiment triggered on $e - p$ coincidences between the HRS spectrometers, with the BigBite and HAND detectors read out for every trigger.

The recoiling protons were detected by the BigBite spectrometer [13] centered at an angle of 97° for the 500 and 625 MeV/$c$ measurements and 92° for the 750 MeV/$c$ measurement. The angle between $\vec{q}$ and the recoil nucleon was 40°–50°. The angular acceptance was about 96 msr and the detected momenta accepted ranged from 0.25 to 0.90 GeV/$c$. The momentum resolution of BigBite, determined from elastic electron-proton scattering, was $\Delta p/p = 1.5\%$. The overall proton detection efficiency was $73 \pm 1\%$.

HAND consists of several elements: a 2.4-cm-thick lead shield (to block low-energy photons and most of the charged particles coming from the target), followed by 64, 2-cm-thick scintillators (to identify and veto charged particles), and 112 plastic scintillator bars arranged in six, 10-cm-thick layers covering an area of $1 \times 3$ m$^2$ (to detect the neutrons). HAND was placed six meters from the target, just behind BigBite, covering a similar solid angle as BigBite.

The pattern of hits in sequential layers of HAND was used to identify neutrons [14]. A time resolution of 1.5 ns allowed determination of the neutron momentum with an accuracy that varied from 2.5% (at 400 MeV/$c$) to 5% (at 830 MeV/$c$). The detection efficiency was $40 \pm 1.4\%$ for 400–830 MeV/$c$ neutrons. This determination is based on the
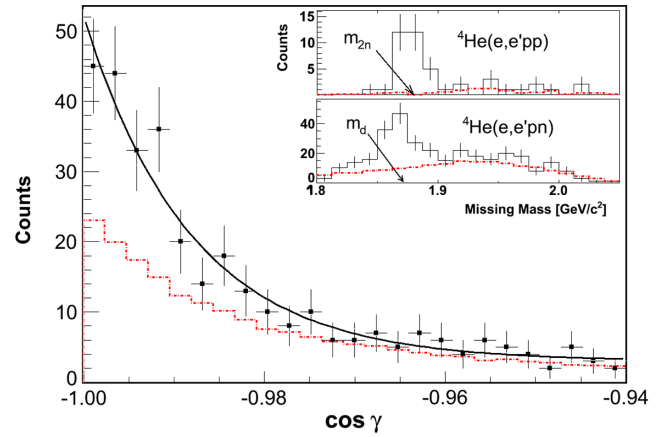


FIG. 1 (color online). The distribution of the cosine of the opening angle $\gamma$ between the $\vec{p}_{\text{miss}}$ and $\vec{p}_{\text{recoil}}$ for the $^4$He$(e, e'pn)$ reaction ($p_{\text{miss}} = 625$ and 750 MeV/$c$ kinematics combined). The solid curve is a simulation of scattering off a moving pair with a c.m. momentum having a width of 100 MeV/$c$. The inserts show the missing-mass distributions. In both the main figure and the inserts, the data are shown with no random background subtraction. The random background is shown as dash-dotted (red online) curves.

efficiency measured up to 450 MeV/$c$ using the $d(e, e'pn)$ reaction, and extrapolated using a simulation that reproduces well the measured efficiency at lower momenta [15].

The picture of SRC pair breakup with the other two nucleons in $^4$He being essentially spectators is supported by Fig. 1. The figure shows the distribution of the cosine of the angle between the missing momentum and the recoiling neutrons ($\gamma$). We also show the angular correlation for the random background (dashed-dotted) as defined by a time window off the coincidence peak. While the placement of the neutron detector opposite to the nominal missing momentum defined by the central rays of the high resolution spectrometers leads to a geometrical angular correlation in the random background, the real triple-coincidence events show a clear back-to-back peak above this background. The curve is a result of a simulation of the scattering of a moving pair as discussed below. Similar back-to-back correlations were observed for the recoiling protons. The inserts to Fig. 1 show the missing-mass for the $^4$He$(e, e'pp)$ and $^4$He$(e, e'pn)$ reactions corresponding to a two-nucleon residual system with a low-excitation energy.

Software cuts were applied to both BigBite and HAND that limited their acceptances to $\pm 14°$ in the vertical direction, $\pm 4°$ in the horizontal direction, and 300–900 MeV/$c$ in momentum. A model, tuned to match experimental data, was used to correct the yield of the $^4$He$(e, e'pN)$ events for the finite acceptances of the recoiling protons and neutrons in BigBite and HAND. Following Ref. [1], the simulations assumed that an electron scatters off a moving SRC pair with a c.m. momentum relative to the $A - 2$ spectator system described by a Gaussian distribution as in Ref. [16]. We assumed an

isotropic three-dimensional motion of the pair and varied the width of the Gaussian equally in each direction until the best agreement with the data was obtained. The nine measured distributions (three components in each of the three kinematic settings for $np$ pairs) yield, within the uncertainties, the same width with a weighted average of $100 \pm 20$ MeV/$c$. This is in good agreement with the c.m. momentum distribution calculated in Ref. [10]. Figure 1 compares the simulated and measured distributions of the opening angle between the knocked-out and recoiling nucleons. The fraction of events detected within the finite acceptance was used to correct the measured yield. The uncertainty in this correction was typically 15%, which dominates the systematic uncertainties of the $^4$He$(e, e'pN)$ yield.

The measured $^4$He$(e, e'pN)/^4$He$(e, e'p)$ ratios are given by the number of events in the background-subtracted triple-coincidence TOF peak corrected for the finite acceptance and detection efficiency of the recoiling nucleons, divided by the number of random-subtracted (double-coincidence) $^4$He$(e, e'p)$ events. These ratios, as a function of $p_{\text{miss}}$ in the $^4$He$(e, e'p)$ reaction, are displayed as full symbols in the two upper panels of Fig. 2. Because the electron can scatter from either proton of a $pp$ pair (but only from the single proton of an $np$ pair), we divided the $^4$He$(e, e'pp)$ yield by two. Also displayed in Fig. 2, as empty symbols with dashed bars, are similar ratios for $^{12}$C obtained from previous electron scattering [1,2] and proton scattering [4] measurements. In comparing the $^{12}$C and $^4$He data, it is noted that the measured ratios are about equal and very different from the ratios of naive pair counting in these nuclei. The horizontal bars show the overlapping momentum acceptance ranges of the various kinematic settings. The vertical bars are the uncertainties, which are predominantly statistical.

Because we obtained the $^4$He$(e, e'pp)$ and $^4$He$(e, e'pn)$ data simultaneously and with the same solid angles and momentum acceptances, we could also directly determine the ratio of $^4$He$(e, e'pp)$ to $^4$He$(e, e'pn)$. In this ratio, many of the systematic factors needed to compare the triple-coincidence yields cancel out, and we need to correct only for the detector efficiencies. This ratio as a function of the missing momentum is displayed in the bottom panel of Fig. 2 together with the previously measured ratio for $^{12}$C [2].

To extract from the measured cross-section ratios the underlying pair ratios, corrections for final-state interactions (FSI) were calculated using the Glauber approximation [17]. The Glauber corrections ($T_L = 0.75$ and $T_R = 0.66$–$0.73$), with $T_L$ and $T_R$ the leading and recoil transparencies, were calculated by the Ghent group [17]. We assumed the uncertainties to be $\pm 20\%$ of these values. The single charge exchange (SCX) probability ($P_{\text{SCX}}$) was assumed to be $1.5 \pm 1.5\%$ based on the SCX total cross section of $1.1 \pm 0.2$ mb [18]. The pair fraction extracted from the measured ratios with the FSI calculated corrections are shown in Fig. 2 as bands (see the Appendix for
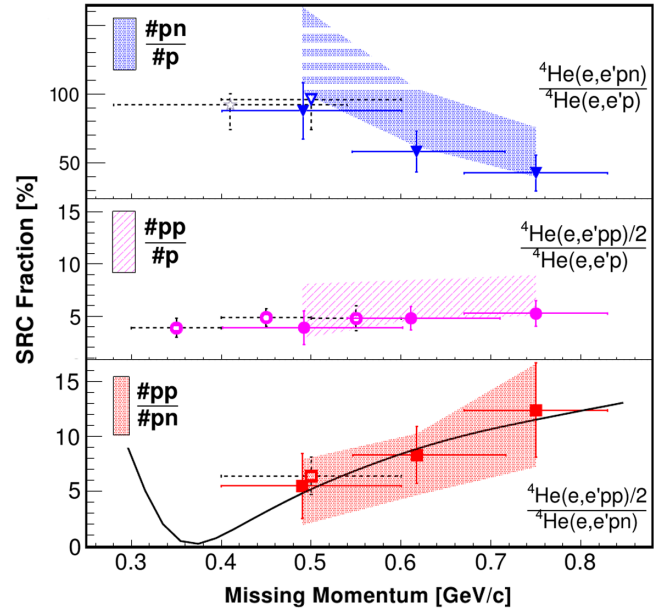


FIG. 2 (color online). Bottom panel: the measured ratios $^4$He$(e, e'pp)/^4$He$(e, e'pn)$ shown as solid symbols, as a function of the $^4$He$(e, e'p)$ missing momentum. Each point is the result of a different setting of the detectors. The bands represent the data corrected for FSI to obtain the pair ratios, see text for details. Also shown are calculations using the momentum distribution of Ref. [10] for pairs with weighted-average c.m. momentum assuming arbitrary angles between the c.m. and the relative momenta in the pair (solid black line). The middle panel shows the measured $^4$He$(e, e'pp)/^4$He$(e, e'p)$ and extracted #$pp$/#$p$ ratios. The top panel shows the measured $^4$He$(e, e'pn)/$$^4$He$(e, e'p)$ and extracted #$pn$/#$p$ ratios. The unphysical region above 100% obtained due to systematic uncertainties and statistical fluctuations is marked by white strips. Ratios for $^{12}$C are shown as empty symbols with dashed bars. The empty star in the top panel is the BNL result [4] for $^{12}$C$(p, 2pn)/^{12}$C$(p, 2p)$.

details). The statistical and systematic uncertainties were treated as independent and combined by simulation to create the width of the one standard deviation bands shown in Fig. 2. The systematic uncertainties in the correction factor (15% due to finite detector acceptance, $\sim 20\%$ due to FSI) and statistical fluctuations can explain the extension of the band beyond 100%.

The correction to the ratios due to attenuation of the leading-proton is small. The attenuation of the recoiling nucleon decreases the measured triple- or double-coincidence ratios. Because the measured $^4$He$(e, e'pn)$ rate is about an order of magnitude larger than the $^4$He$(e, e'pp)$ rate, $^4$He$(e, e'pn)$ reactions followed by a single charge exchange [and hence detected as $^4$He$(e, e'pp)$] increase the $^4$He$(e, e'pp)/^4$He$(e, e'pn)$ and the $^4$He$(e, e'pp)/^4$He$(e, e'p)$ measured ratios.

The two-nucleon momentum distributions were calculated for the ground states of $^4$He using variational Monte Carlo wave functions derived from a realistic Hamiltonian

with Argonne V18 and Urbana X potentials [10]. The calculations for fixed pair c.m. momentum ($K_{\text{c.m.}}$) averaged over all directions of the relative momentum ($\vec{K}_{\text{rel}}$) and $\vec{K}_{\text{c.m.}}$ [10] were weighted by the measured distribution of $K_{\text{c.m.}}$ to yield the solid (black) curve shown in Fig. 2. The calculation with $K_{\text{c.m.}} = 0$, which agrees quantitatively with the Perugia group calculation [19], differs little from the average shown in the figure. To compare the calculations to the data in Fig. 2 we assumed that the virtual photon hits the leading proton and that $\vec{p}_{\text{miss}} = \vec{K}_{\text{rel}}$ (plane wave impulse approximation).

The measurements reported here were motivated by the attempt to study the isospin decomposition of SRC as a proxy to a transition from primarily tensor to the short range repulsive, presumably scalar, nucleon-nucleon force. In the ground state of $^4$He [10], the number of $pp$-SRC pairs is much smaller than $np$-SRC pairs for values of the relative nucleon momentum $K_{\text{rel}} \approx 400$ MeV/$c$. This is because the correlations induced by the tensor force are strongly suppressed for $pp$ pairs which are predominantly in $^1S_0$ state [8–10,19]. As the relative momenta increase, the tensor force becomes less dominant, the role played by the short-range repulsive force increases and with it the ratio of $pp/np$ pairs. In our measurement, as the missing momenta is increased beyond 500 MeV/$c$, the triple-coincidence $^4$He$(e, e'pp)/^4$He$(e, e'pn)$ ratio increases, in good agreement with the prediction based on the ratio of $pp$-SRC/$np$-SRC pairs in the $^4$He ground state [10].

The measured triple/double coincidence ratios shed further light on the dynamics. The measured $^4$He$(e, e'pp)/$ $^4$He$(e, e'p)$ ratio reflects a small contribution from $pp$-SRC pairs. These pairs are likely dominated by a scalar repulsive short-range force which is relatively constant over the reported momentum range.

The $^4$He$(e, e'pn)/^4$He$(e, e'p)$ ratio clearly shows that the reduction in the $np/pp$ ratio with increasing $p_{\text{miss}}$ is due to a drop in $np$-SRC pairs with increasing $K_{\text{rel}}$. While $np$ pairs still dominate SRC, even at missing momentum of 800 MeV/$c$, the total fraction of the $(e, e'p)$ cross section associated with scattering from SRC pairs drops with increasing missing momentum. This is likely due to an increase of more complex mechanisms, such as stronger FSI and the onset of SRC involving more than two nucleons [5]. A definitive understanding of the relative importance of these effects requires exclusive measurements at large missing momentum on heavier nuclei, and a more detailed theoretical study.

To summarize, the short range part of the $NN$ force is empirically known to be repulsive, it is essential to describe $NN$ scattering and stability of nuclei, but it is difficult to explore and poorly known both theoretically and experimentally. The measurements reported here probe a transition from an attractive to a repulsive $NN$ force. The data set, interpreted as changes in the isospin decomposition of the SRC pairs, is consistent with a reduced contribution

from a tensor component and a constant contribution from a scalar component of the $NN$ force over the probed missing momentum range. It confirms the phenomenological description of the $NN$ force in this range.

One should question to what level the naive interpretation of the data in terms of the ground state nuclear properties is appropriate. Comprehensive calculations, which take into account the full reaction mechanism in a relativistic treatment, as well as additional data with better statistics will allow a more detailed determination of the role played by the elusive repulsive short-range nucleon-nucleon interaction.

*Appendix.*—To extract the SRC pair ratios ($\#pp/\#np$, $\#pp/\#p$, and $\#np/\#p$) from the measured cross-section ratios [$R = (^4$He$(e, e'pp)/^4$He$(e, e'pn))$, $R_1 = (^4$He$(e, e'pn)/^4$He$(e, e'p))$, $R_2 = (^4$He$(e, e'pp)/$ $^4$He$(e, e'p))$], we assumed factorization and used Eqs. (A.1–A.3),

$$\frac{\#pp}{\#np} = \frac{T_L R - P_{\text{SCX}} \frac{\sigma_{en}}{\sigma_{ep}}}{2T_L - 2P_{\text{SCX}} \frac{\sigma_{en}}{\sigma_{ep}} R} \tag{A1}$$

$$\frac{\#pp}{\#p} = \frac{R_1 \frac{\sigma_{en}}{\sigma_{ep}} \frac{P_{\text{SCX}}}{T_L} T_R - R_2 T_R}{2(\frac{\sigma_{en}}{\sigma_{ep}} \frac{P_{\text{SCX}}}{T_L} T_R)^2 - 2T_R^2} \tag{A2}$$

$$\frac{\#np}{\#p} = \frac{R_2 - 2\frac{\#pp}{\#p} T_R}{\frac{\sigma_{en}}{\sigma_{ep}} \frac{P_{\text{SCX}}}{T_L} T_R}, \tag{A3}$$

where $\sigma_{ep}$ ($\sigma_{en}$) is the cross section for electron scattering off the proton (neutron) [20].

* deceased

[1] R. Shneor *et al.*, Phys. Rev. Lett. **99**, 072501 (2007).
[2] R. Subedi *et al.*, Science **320**, 1476 (2008).
[3] A. Tang *et al.*, Phys. Rev. Lett. **90**, 042301 (2003).

[4] E. Piasetzky, M. Sargsian, L. Frankfurt, M. Strikman and J. W. Watson, Phys. Rev. Lett. **97**, 162504 (2006).

[5] L. L. Frankfurt and M. I. Strikman, Phys. Rep. **76**, 215 (1981).

[6] L. L. Frankfurt and M. I. Strikman, Phys. Rep. **160**, 235 (1988).

[7] J. Arrington, D. W. Higinbotham, G. Rosner, and M. Sargsian, Prog. Part. Nucl. Phys. **67**, 898 (2012).

[8] R. Schiavilla, R. B. Wiringa, S. C. Pieper, and J. Carlson, Phys. Rev. Lett. **98**, 132501 (2007).

[9] R. B. Wiringa, R. Schiavilla, S. C. Pieper and J. Carlson, Phys. Rev. C **78**, 021001 (2008).

[10] R. B. Wiringa, R. Schiavilla, S. C. Pieper, and J. Carlson, Phys. Rev. C **89**, 024305 (2014).

[11] J. Alcorn *et al.*, Nucl. Instrum. Methods Phys. Res., Sect. A **522** (2004) 294.

[12] P. Monaghan, Ph.D. thesis, MIT, 2008.

[13] M. Mihovilovič *et al.*, Nucl. Instrum. Methods Phys. Res., Sect. A **686**, 20 (2012).

[14] R. Subedi, Ph.D. thesis, Kent State University, 2007.

[15] R. A. Cecil, B. D. Anderson and R. Madey, Nucl. Instrum. Methods **161**, 439 (1979).

[16] C. Ciofi degli Atti and S. Simula, Phys. Rev. C **53**, 1689 (1996).

[17] J. Ryckebusch, D. Debruyne, P. Lava, S. Janssen, B. Van Overmeire, and T. Van Cauteren, Nucl. Phys. **A728**, 226 (2003); W. Cosyn, M. C. Martinez and J. Ryckebusch, Phys. Rev. C **77**, 034602 (2008); W. Cosyn and J. Ryckebusch (private communication).

[18] J. L. Friedes, H. Palevsky, R. L. Stearns, and R. J. Sutter, Phys. Rev. Lett. **15**, 38 (1965).

[19] M. Alvioli, C. Ciofi degli Atti, L. P. Kaptari, C. B. Mezzetti, H. Morita, and S. Scopetta, Phys. Rev. C **85**, 021001(R) (2012); C. Ciofi degli Atti and H. Morita (private communication).

[20] S. Rock, R. Arnold, P. Bosted, B. Chertok, B. Mecking, I. Schmidt, Z. Szalata, R. York, and R. Zdarko, Phys. Rev. Lett. **49**, 1139 (1982).